IEEE Access
Multidisciplinary ⋮ Rapid Review ⋮ Open Access Journal

Received November 30, 2020, accepted December 21, 2020, date of publication December 28, 2020,
date of current version January 8, 2021.

Digital Object Identifier 10.1109/ACCESS.2020.3047810

Novel Sliding Mode Vibration Controller With Simple Model-Free Design and Compensation for Actuator's Uncertainty

ANSEI YONEZAWA, ITSURO KAJIWARA, AND HEISEI YONEZAWA
Division of Human Mechanical Systems and Design, Hokkaido University, Sapporo 060-8628, Japan

Corresponding author: Itsuro Kajiwara (ikajiwara@eng.hokudai.ac.jp)

This work was supported by the Japan Society for the Promotion of Science, Grants-in-Aid for Scientific Research (B), under Project JP19H02088 and Grant JP 20J11084.

ABSTRACT This study proposes an active vibration control method with a simple design process without using a plant model. The proposed method is robust against the actuator's parameter uncertainty. To realize model-free control of the controlled object, a virtual structure represented by a single-degree-of-freedom system is inserted between the controlled object and the actuator. A controller, which compensates for the uncertainties of the actuator's parameters, is designed using the sliding mode control theory. By designing a controller using a model composed of the virtual structure and the actuator, model-free design can be easily performed with few design variables. After the virtual structure is introduced, the controller can be designed using the same process as a traditional model-based control theory. An advantage of the sliding mode control system is it can provide high robustness against the uncertainty in the actuator's parameters. The robustness to the actuator's uncertainty and vibration suppression performance of the proposed method are verified by controlling a two-degree-of-freedom time-varying system. Finally, the applicability of the proposed method to an actual mechanical system is confirmed by vibration control experiments.

INDEX TERMS Model-free control, active vibration control, virtual structure, sliding mode control, proof-mass actuator, actuator uncertainty, robust control, time-varying system.

I. INTRODUCTION

Vibration control technologies have become increasingly important to improve performance, downsize, and reduce the weight of mechanical systems in recent years. Active vibration control, which can obtain high vibration suppression performance, is widely studied [1], [2]. Many theories and control techniques have been applied to complex vibration problems, including classical control theory such as PID control, modern control theory such as linear quadratic regulators, as well as adaptive control and model predictive control [3], [4].

Mathematical modeling of a controlled object is usually necessary to design a controller for active vibration control. Hence, the individual controlled objects must be modeled, which is a burdensome and costly process. Moreover, the damping performance and stability of a controller designed based on a mathematical model of the controlled object largely depends on the model's accuracy. Therefore, model-based vibration control is fragile to model changes and modeling errors, which always exist in actual mechanical systems.

Many studies have investigated active vibration control systems that do not require mathematical models of controlled objects [5]–[8]. For example, one study proposed constructing a vibration control system based on the physical insight of the dynamics for semi-active suspension [9].

The model-free vibration control approaches achieved by using online calculation technique were proposed [10]–[15]. In addition, one research group applied a feedback controller based on simultaneous perturbation stochastic approximation for noise reduction of periodic disturbances in a duct [16]. Nevertheless, vibration control using real-time optimization has a large computational load. Consequently, such approaches are not suitable for practical implementation.

The associate editor coordinating the review of this manuscript and approving it for publication was Mou Chen.

This work is licensed under a Creative Commons Attribution 4.0 License. For more information, see https://creativecommons.org/licenses/by/4.0/

Model-free control based on a data-driven control method has been widely studied [17], [18]. This approach constructs the controller using input and output data of the plant. For example, a data-driven control approach using a Taylor series and the differential mean value theorem for a discrete-time nonlinear system has been proposed [19]. However, the data-driven control method has numerous tuning parameters and imposes a heavy calculation burden.

One effective way to realize a model-free control system is to introduce neural networks (NNs) [20]–[26]. Vibration control for a flexible cantilever using a neurocontroller trained by emulator neural networks was proposed for a structure system [27]. However, the controller design procedure using NNs requires enormous training data to learn vibration control, which places a heavy burden on the designer.

Fuzzy control provides if-then–type control rules obtained by fuzzy sets, which express ambiguous information about the plant such as empirical knowledge. Because this approach does not require accurate mathematical models of plants, model-free controller design can be established [28]–[31]. For example, vibration control of a building structure using a PI/PID controller combined with a fuzzy controller to compensate for the nonlinear restoring force was proposed [32]. Fuzzy controller design lacks systematic approaches to set control rules and membership functions. Because it largely depends on designer's experiences and insight, the burden on the designer is huge.

Collectively, these previous studies provide few simple and practical model-free vibration control methods with a small burden on designers. The authors proposed a vibration controller design procedure using only an actuator model and virtual structure model defined as a single-degree-of-freedom (SDOF) system to achieve this goal [33], [34]. However, an actuator has parameter uncertainty due to individual differences in production and deterioration with age due to long-term use. This uncertainty heavily affects the stability and control performance. In model-free vibration control using a virtual structure, traditional matured model-based control theory can be applied directly after the virtual structure is introduced. Therefore, using H_∞ control theory as a typical linear robust control theory, the actuator's parameter uncertainty compensation in model-free vibration control using a virtual structure was proposed [35]. Depending on the amount and type of uncertainty to be compensated, the controller designed by H_∞ control theory becomes too conservative to obtain a sufficient damping performance.

Sliding mode control (SMC) is a control method to stabilize the system by binding the state of the system to a sliding surface, which is a set of the system's desired dynamics. As noteworthy advantage of SMC, when the state of the system is on the sliding surface, the system becomes invariant to the disturbances and uncertainties which satisfies the matching condition [36]. Nevertheless, the uncertainties and disturbances existing in many practical systems do not match the matching condition, making it difficult to utilize the advantages of SMC [37], [38]. On the other hand, the actuator's parameter uncertainty in the model-free vibration control system using the virtual structure proposed in this study satisfies the matching condition. Therefore, employing SMC to compensate for the actuator's parameter uncertainty in a model-free vibration control system using the virtual structure is very effective. Incidentally, in addition to conventional SMC, various approaches to compensate for such parametric uncertainties were proposed. For example, asymptotic tracking control of hydraulic actuation system using adaptive recursive robust integral of sign of the error (RISE) control was conducted [39] and extended state observer (ESO) based adaptive controller was constructed for electrohydraulic servomechanism [40]. These are innovative methods that can be applied to highly nonlinear systems and systems that are difficult to be handled in a conventionally robust control framework. However, they are model-based control methods that design the controller using the models or parameters of the controlled object. On the other hand, this study differs from the previous studies and proposes a model-free SMC designed without using any mathematical models of controlled objects.

This study constructs a model-free vibration control method with a simple controller design procedure and high robustness to the actuator's parameter uncertainty. The proposed method accomplishes the model-free design procedure using the virtual structure and compensates the actuator's parameter uncertainty using SMC. Specifically, the model-free control system is constructed by inserting virtual structure between the actual controlled object and actuator, and setting appropriate parameters considering the frequency transfer characteristics. Then the actuator's parameter uncertainty is modeled using the constructed control system. The uncertainty matches the matching condition of SMC. Based on SMC theory and the Lyapunov function method, a model-free controller with robustness against the actuator's uncertainty is designed without using any parameters of the controlled object. From the above, a controller that does not use any parameters of the actual controlled object and that compensates for the uncertainty of the actuator is designed. By designing the controller using a system composed of the actuator and the SDOF virtual structure, model-free controller design is established with a few design variables. In addition, after introducing the virtual structure, the controller can be designed using the exact same process as traditional model-based controller design. Moreover, actuator's uncertainty is considered and sufficient vibration suppression performance can be obtained by using SMC system's matching condition. The effectiveness of the proposed method is verified by both simulations and experiments. First, the robustness to the actuator's parameter uncertainty is confirmed by conducting a vibration control simulation to a two-degree-of-freedom (2DOF) system with time-varying mass. The effectiveness of the proposed method to an actual mechanical system is subsequently confirmed via a vibration control experiment to both ends

supported plate and cantilever plate as a typical continuous structure. In addition, by the vibration control experiments, the proposed model-free SMC was compared with a conventional model-based SMC. As a result, the advantage (i.e. the robustness against a changing of a controlled object) of the model-free controller design approach based on the idea of virtual structure was confirmed.

Compared to the existing SMC [36] and our previous study [35], the contributions and technical novelties of the proposed control system are indicated as follows.

1) The proposed sliding mode controller becomes a model-free controller, which can be designed without using any models of controlled objects and any those parameters at all. Specifically, the idea of introducing a virtual structure into the actuator is the technical contribution that enables the model-free SMC. In the proposed approach, the clear design condition determines the virtual structure model, and then SMC is designed for the low-order state equation including it instead of an actual plant model. Furthermore, compared to the traditional model-free design methods such as NNs and fuzzy inference, the proposed approach realizes a simpler implementation of the vibration controller without the complicated processes.
2) The compensation for actuator's parameter uncertainty can be achieved simultaneously with the model-free controller design indicated in contribution 1. Although the proposed method uses no models of actual controlled objects to design the control system, the actuator model is required. In our previous work [35], the actuator uncertainty was addressed by the H_∞ controller. On the other hand, the contribution of this paper is the application of SMC to the issue. A noteworthy point of the model-free control system using virtual structure is that the actuator parameter's uncertainty satisfies the matching condition when applying SMC. Therefore, the damping performance can be improved by eliminating conservativeness of H_∞ control. Note that the application of SMC to compensate for actuator uncertainty is based on the model-free controller design via virtual structure.

In other words, the technical novelty of contributions 1. and 2. is the combination of our proposed model-free design via virtual structure and the existing SMC. Therefore, the proposed approach is fundamentally different from the existing model-based SMC and the traditional model-free design methods. In addition, because the actuator uncertainty is addressed by SMC, this paper advances our previous work employing H_∞ control from the viewpoint of enhancement of robustness. Compared to the traditional model-free approaches such as NNs and fuzzy inference, the proposed method, which derives a controller simply by using the virtual structure instead of actual plant models, does not require the complicated design processes with a lot of time and preparations.

II. SYSTEM FOR DESIGNING A MODEL-FREE CONTROLLER

A. DERIVING THE STATE EQUATION FOR MODEL-FREE CONTROL

Fig. 1 shows the actuator employed in this study. It is a proof-mass electromagnetic actuator that can be modeled as a SDOF system due to its mechanical characteristics [34].

Here, model-free active vibration control is established by inserting a virtual structure defined as a SDOF system between the actuator and the controlled object [33]–[35]. Fig. 2(a) shows the actual mechanical system model. The parameters m, k and c indicate the mass, stiffness, and damping of the model, respectively. Subscripts 0 and 1 denote the actuator model and the controlled object, respectively. The structure of the controlled object is arbitrary. The aim is to suppress the vibration of the actual controlled object x_1 using the control input u generated by the actuator.

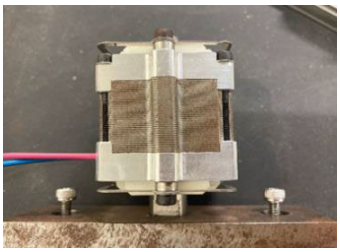

FIGURE 1. Proof-mass electromagnetic actuator.

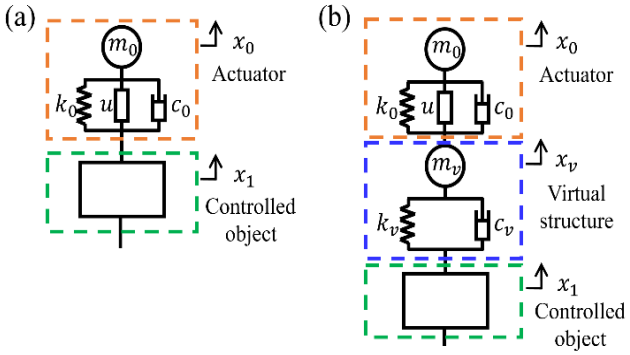

FIGURE 2. Models for control system design: (a) Actual system; (b) System with a virtual structure.

Fig. 2(b) shows the model in which a virtual structure is inserted between the actuator and the actual controlled object for model-free controller design. Subscript v represents the virtual structure. The basic concept to realize model-free control is to regard the virtual structure as a controlled object and to indirectly suppress the vibration of the actual controlled object x_1 by quashing the vibration of the virtual structure x_v. The controller can be obtained easily by applying traditional model-based control theory directly to a 2DOF system composed of the actuator and the virtual structure.

The equations of motion with respect to m_0 and m_v in Fig. 2(b) can be written as

$$m_0\ddot{x}_0 + c_0(\dot{x}_0 - \dot{x}_v) + k_0(x_0 - x_v) = u \quad (1)$$

$$m_v\ddot{x}_v + c_v(\dot{x}_v - \dot{x}_1) + k_v(x_v - x_1) + c_0(\dot{x}_v - \dot{x}_0) + k_0(x_v - x_0) = -u \quad (2)$$

The transfer characteristic T_{xvx1} from x_1 to x_v is obtained as (3) by Laplace transform when c_v is set to 0 in (1) and (2). Here, s is the Laplace operator, and the Laplace transformed functions are written in capital letters.

$$T_{xvx1} = \frac{X_v(s)}{X_1(s)} = \frac{(m_0s^2 + c_0s + k_0)k_v}{\{m_vs^2 + c_0s + (k_0 + k_v)\}(m_0s^2 + c_0s + k_0) - (c_0s + k_0)^2} \quad (3)$$

The parameters of the virtual structure are adjusted as design variables. In (3), the transfer characteristic T_{xvx1} converges to 1 by setting the virtual structure's parameters to $k_v \to \infty$ and $m_v = 0$. In other words, the vibration of the virtual structure becomes the same as that of the actual controlled object. Consequently, indirect vibration suppression of the controlled object is achieved by suppressing the vibration of the virtual structure. On the other hand, k_v must be a finite positive value and m_v cannot be 0 since the controller is derived by a numerical calculation. Therefore, the aim is to establish the transfer characteristic approximately as

$$T_{xvx1} \approx 1 \quad (4)$$

Equation (4) is satisfied when k_v is set to a sufficiently large positive finite value, and m_v is a sufficiently small positive finite value. Table 1 shows the values of the actuator and virtual structure employed in this study.

TABLE 1. Parameters for control system design.

Properties	Value	Unit
m_0	0.2013	kg
k_0	3518	N/m
c_0	1.186	Ns/m
m_v	1.0×10^{-5}	kg
k_v	7.0×10^5	N/m
c_v	0.0	Ns/m

In (1) and (2), to derive a state equation for designing the model-free controller, disturbance w is defined as

$$w = c_v\dot{x}_1 + k_vx_1 \quad (5)$$

This leads to the 2DOF state equation shown in (6)–(8).

$$\dot{x}_{va} = A_{va}x_{va} + B_{va1}w + B_{va2}u \quad (6)$$

$$x_{va} = \begin{bmatrix} x_v & x_0 & \dot{x}_v & \dot{x}_0 \end{bmatrix}^T \quad (7)$$

$$A_{va} = \begin{bmatrix} 0 & 0 & 1 & 0 \\ 0 & 0 & 0 & 1 \\ -\dfrac{k_0 + k_v}{m_v} & \dfrac{k_0}{m_v} & -\dfrac{c_0 + c_v}{m_v} & \dfrac{c_0}{m_v} \\ \dfrac{k_0}{m_0} & -\dfrac{k_0}{m_0} & \dfrac{c_0}{m_0} & -\dfrac{c_0}{m_0} \end{bmatrix}$$

$$B_{va1} = \begin{bmatrix} 0 & 0 & \dfrac{1}{m_v} & 0 \end{bmatrix}^T$$

$$B_{va2} = \begin{bmatrix} 0 & 0 & -\dfrac{1}{m_v} & \dfrac{1}{m_0} \end{bmatrix}^T \quad (8)$$

Equation (6) does not contain any parameters of the actual controlled object. Consequently, model-free vibration control can be achieved by designing the controller to the (6), which regards the virtual structure as the controlled object. Consequently, the designed controller can suppress the actual controlled object's vibration indirectly by satisfying (4).

In feedback control applied to the above system, vibration control is achieved by feeding the vibration of the virtual structure back as an observed output. However, the actual system does not contain a virtual structure. Therefore, in actual feedback control, the observed output is the vibration of the actual controlled object x_1, which is almost the same as x_v by (4).

B. DESIGN OF THE VIRTUAL STRUCTURE

Equation (4) is established in a limited frequency band since the parameters of the virtual structure are not allowed to be settled as $k_v \to \infty$ and $m_v = 0$. Therefore, in the controlled frequency band, the virtual structure must be designed to satisfy (4). In this study, the virtual structure is designed by design condition (9) proposed in a previous study [34]. The lower and upper limited frequencies of the controlled frequency band are written as Ω_1^{cont} and Ω_2^{cont} ($\Omega_2^{cont} > \Omega_1^{cont} \geq \sqrt{k_0/m_0}$), respectively.

$$\left\{\left(\frac{(\Omega_k^{cont})^2}{k_0} - \frac{1}{m_0}\right)k_v + (\Omega_k^{cont})^2\right\}\frac{1}{m_v} > \left(\frac{(\Omega_k^{cont})^2}{k_0} - \frac{1}{m_0}\right)(\Omega_k^{cont})^2 \quad (k = 1, 2) \quad (9)$$

Fig. 3 shows the Bode diagram of the transfer characteristic $T_{xvx1}(s)$. In $f \in (f_1 \cong 20.6\text{Hz}, f_2 \cong 7.03 \times 10^3\text{Hz})$, which includes the controlled band, the gain can be regarded as 1 and the phase can be regarded as 0°. Consequently, (4) is satisfied.

III. SLIDING MODE CONTROLLER DESIGN

A. MODELING OF THE ACTUATOR'S PARAMETER UNCERTAINTY

A model-free vibration control system can be constructed when (6) includes the actuator's parameter uncertainty. This study considers the uncertainties of the actuator's stiffness and damping. The actuator's parameters with uncertainty are expressed as (10) [35].

$$k_{0m} = k_{0n} + \Delta_k k_e, \quad -1 \leq \Delta_k \leq 1$$
$$c_{0m} = c_{0n} + \Delta_c c_e, \quad -1 \leq \Delta_c \leq 1 \quad (10)$$

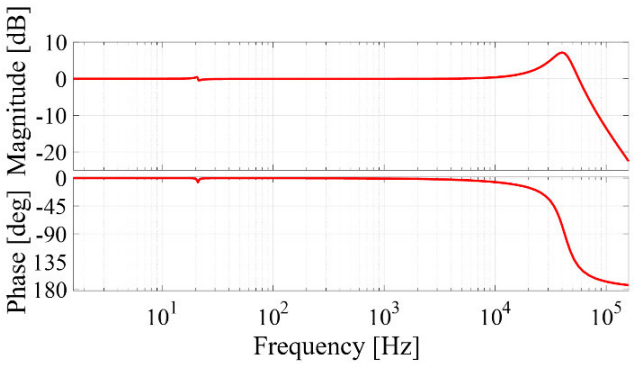

FIGURE 3. Transfer property from x_1 to x_v.

Here, k_{0m} and c_{0m} are the actual values of k_0 and c_0, which include uncertainties with values shown in Table 1. k_{0n} and c_{0n} are the nominal values of k_0 and c_0, and they are the same as those in Table 1. Δ_k and Δ_c are normalized fluctuations. k_e and c_e, which are the maximum amounts of errors to be compensated, are defined when the controller is designed. Consequently, due to (10), the actual stiffness k_{0m} and damping c_{0m} of the actuator are expressed as uncertain values given by the nominal values k_{0n} and c_{0n} with maximum fluctuations $\pm k_e$ and $\pm c_e$. Equations (11)–(13) are derived by substituting k_{0m} and c_{0m} into k_0 and c_0 of (6)–(8) and setting c_v as 0. In (11), $\Delta A x_{va}$ represents the effect of the actuator's uncertainty.

$$\dot{x}_{va} = (A_{vn} + \Delta A)x_{va} + B_{v1}w + B_{v2}u \tag{11}$$

$$x_{va} = \begin{bmatrix} x_v & x_0 & \dot{x}_v & \dot{x}_0 \end{bmatrix}^T \tag{12}$$

$$A_{vn} = \begin{bmatrix} 0 & 0 & 1 & 0 \\ 0 & 0 & 0 & 1 \\ -\dfrac{k_{0n}+k_v}{m_v} & \dfrac{k_0}{m_v} & -\dfrac{c_{0n}}{m_v} & \dfrac{c_{0n}}{m_v} \\ \dfrac{k_{0n}}{m_0} & -\dfrac{k_{0n}}{m_0} & \dfrac{c_{0n}}{m_0} & -\dfrac{c_{0n}}{m_0} \end{bmatrix}$$

$$\Delta A = \begin{bmatrix} 0 & 0 & 0 & 0 \\ 0 & 0 & 0 & 0 \\ -\dfrac{\Delta_k k_e}{m_v} & \dfrac{\Delta_k k_e}{m_v} & -\dfrac{\Delta_c c_e}{m_v} & \dfrac{\Delta_c c_e}{m_v} \\ \dfrac{\Delta_k k_e}{m_0} & -\dfrac{\Delta_k k_e}{m_0} & \dfrac{\Delta_c c_e}{m_0} & -\dfrac{\Delta_c c_e}{m_0} \end{bmatrix}$$

$$B_{va1} = \begin{bmatrix} 0 & 0 & \dfrac{1}{m_v} & 0 \end{bmatrix}^T$$

$$B_{va2} = \begin{bmatrix} 0 & 0 & -\dfrac{1}{m_v} & \dfrac{1}{m_0} \end{bmatrix}^T \tag{13}$$

B. SLIDING SURFACE DESIGN

Sliding surface $\sigma = 0$ is designed to the system and switching function σ represented as (14)–(17) so that the fluctuation of the state of the system x_{va} is minimized on the sliding surface [36]. Equations (14)–(16) represent (11)–(13) without the disturbance w and actuator's uncertainty $\Delta A x_{va}$. Here, the dimension of B_{22} is equal to that of u in (16).

$$\dot{x}_{va} = A_{vn}x_{va} + B_{v2}u \tag{14}$$

$$x_{va} = \begin{bmatrix} x_v & x_0 & \dot{x}_v & \dot{x}_0 \end{bmatrix}^T \tag{15}$$

$$A_{vn} = \begin{bmatrix} 0 & 0 & 1 & 0 \\ 0 & 0 & 0 & 1 \\ -\dfrac{k_{0n}+k_v}{m_v} & \dfrac{k_0}{m_v} & -\dfrac{c_{0n}}{m_v} & \dfrac{c_{0n}}{m_v} \\ \dfrac{k_{0n}}{m_0} & -\dfrac{k_{0n}}{m_0} & \dfrac{c_{0n}}{m_0} & -\dfrac{c_{0n}}{m_0} \end{bmatrix}$$

$$B_{v2} = \begin{bmatrix} B_{21} \\ B_{22} \end{bmatrix} = \begin{bmatrix} 0 \\ 0 \\ -\dfrac{1}{m_v} \\ \dfrac{1}{m_0} \end{bmatrix} \tag{16}$$

$$\sigma = Sx_{va} \tag{17}$$

Equations (18)–(20) show the system where the coordinate transformed system of (14)–(16) is given by the coordinate transformation matrix T.

$$\begin{bmatrix} \dot{z}_1 \\ \dot{z}_2 \end{bmatrix} = \begin{bmatrix} A_{11} & A_{12} \\ A_{21} & A_{22} \end{bmatrix} \begin{bmatrix} z_1 \\ z_2 \end{bmatrix} + \begin{bmatrix} 0 \\ B_{22} \end{bmatrix} u \tag{18}$$

$$\begin{bmatrix} z_1 \\ z_2 \end{bmatrix} = Tx_{va}, \quad T = \begin{bmatrix} I & -B_{21}B_{22}^{-1} \\ 0 & I \end{bmatrix} \tag{19}$$

$$\begin{bmatrix} A_{11} & A_{12} \\ A_{21} & A_{22} \end{bmatrix} = TA_{vn}T^{-1} \tag{20}$$

For (14)–(16), the quadratic performance index is settled as (21)–(23) [36]. Here, W is a positive-definite symmetric weighting matrix. In addition, t_s is the time when the sliding motion commences.

$$\begin{aligned} J &= \int_{t_s}^{\infty} x_{va}^T W x_{va} dt \\ &= \int_{t_s}^{\infty} (z_1^T \hat{Q}_{11} z_1 + v^T Q_{22} v) dt \end{aligned} \tag{21}$$

$$v = z_2 + Q_{22}^{-1} Q_{12}^T z_1 \tag{22}$$

$$\begin{aligned} \begin{bmatrix} Q_{11} & Q_{12} \\ Q_{21} & Q_{22} \end{bmatrix} &= T^T W T \\ Q_{21}^T &= Q_{12} \\ \hat{Q}_{11} &= Q_{11} - Q_{12}{Q_{22}}^{-1} Q_{12}^T \end{aligned} \tag{23}$$

Equation (24) is obtained by substituting (22) into the first line of (18).

$$\begin{aligned} \dot{z}_1 &= \hat{A}_{11} z_1 + A_{12} v \\ \hat{A}_{11} &= A_{11} - A_{12}{Q_{22}}^{-1} Q_{12}^T \end{aligned} \tag{24}$$

For (21) and (24), v is calculated as (25) to minimize the performance index J. Here, P is a unique positive-definite symmetric solution of the algebraic Riccati equation (26).

$$v = -{Q_{22}}^{-1} A_{12}^T P z_1 \tag{25}$$

$$P\hat{A}_{11} + \hat{A}_{11}^T P - PA_{12}Q_{22}^{-1}A_{12}^T P + \hat{Q}_{11} = 0 \tag{26}$$

For (22) and (25), the switching function σ is designed as (27). In addition, the sliding surface employed in this study is $\sigma = 0$ of (27).

$$\sigma = Sx_{va} = \begin{bmatrix} A_{12}^T P + Q_{12}^T & Q_{22} \end{bmatrix} Tx_{va} \tag{27}$$

C. ACTUATOR'S UNCERTAINTY OF THE MODEL-FREE CONTROL SYSTEM AND MATCHING CONDITION

A unique characteristics of SMC is that the system is invariant with respect to disturbances and uncertainties that satisfy the matching condition when the system is on a sliding surface [36]–[38]. Here, the matching condition of SMC is that f (disturbances and uncertainties of the system) can be represented as (28) by input matrix B.

$$f = Bh \tag{28}$$

In (11)–(13), actuator uncertainty ΔAx_{va} can be represented as (29). In other words, the actuator uncertainty ΔAx_{va} satisfies the matching condition.

$$\begin{aligned} \Delta Ax_{va} &= \begin{bmatrix} 0 \\ 0 \\ -\dfrac{1}{m_v} \\ \dfrac{1}{m_0} \end{bmatrix} \begin{bmatrix} \Delta_k k_e & -\Delta_k k_e & \Delta_c c_e & -\Delta_c c_e \end{bmatrix} x_{va} \\ &= B_{v2} \tilde{A} x \end{aligned} \tag{29}$$

Therefore, when (11)–(13) is on the sliding surface, the system is invariant with respect to the actuator's uncertainty. Hence, high robustness to the uncertainty is expected.

D. CONTROL INPUT DESIGN AND REACHING LAW

The control input is defined as (30) to (11)–(13) [37]. Here, u_l is the linear input and u_{nl} is the nonlinear switching input. Additionally, k is an appropriate gain and α is an appropriate parameter for chattering reduction, which satisfies $0 < \alpha < 1$ [41].

$$\begin{aligned} u &= u_l + u_{nl} \\ &= -(SB_{v2})^{-1} SA_{vn} x_{va} - k\,|\sigma|^{-\alpha}\, sgn(\sigma) \end{aligned} \tag{30}$$

In (11)-(13), the condition for σ to converge to 0 by the control input (30) (i.e. the existence condition of sliding mode) is derived. Herein the Lyapunov function technique is employed [36], [42], [43]. The Lyapunov candidate function of the dynamics of σ is defined as (31). Note that σ is a scalar.

$$V = \frac{1}{2}\sigma^2 > 0 \tag{31}$$

$$\dot{V} = \sigma^T \dot{\sigma} < 0 \quad for\ \forall \sigma \neq 0 \tag{32}$$

Equation (33) is the first-order differentiation of (31).

$$\begin{aligned} \dot{V} &= \sigma^T \dot{\sigma} = \sigma^T S \dot{x}_{va} \\ &= \sigma^T S \left\{ \Delta Ax_{va} + B_{v1} w - kB_{v2}\,|\sigma|^{-\alpha} \frac{\sigma}{|\sigma|} \right\} \end{aligned} \tag{33}$$

Condition (34) must be established for (33) to satisfy (32).

$$sgn(\sigma)\,(S\Delta Ax_{va} + SB_{v1} w) < k' \quad k' = k\,|\sigma|^{-\alpha}\, SB_{v2} \tag{34}$$

For (4), when the parameters of the virtual structure are properly defined along with Section 2.B, w can be written as

$$w = k_v x_1 \approx k_v x_v = k_v \begin{bmatrix} 1 & 0 & 0 & 0 \end{bmatrix} x_{va} \tag{35}$$

Equation (34) can be evaluated as (36) using (35).

$$\begin{aligned} &sgn(\sigma)\,(S\Delta Ax_{va} + SB_{v1} w) \\ &\quad \leq \|S\| \left\{ \sqrt{2\left(\frac{1}{m_v^2} + \frac{1}{m_0^2}\right)\left\{k_e^2 + c_e^2\right\}} + \frac{k_v}{m_v} \right\} \|x_{va}\| \end{aligned} \tag{36}$$

Consequently, for (11)–(13), the control input and the condition for σ to converge to 0 are derived as (37) and (38). Here, k'' is an appropriate constant gain satisfying condition (38).

$$\begin{aligned} u &= -(SB_{v2})^{-1} SA_{vn} x_{va} \\ &\quad - k''\,(SB_{v2})^{-1}\,|\sigma|^{\alpha}\,\|x_{va}\|\, sgn(\sigma) \end{aligned} \tag{37}$$

$$\begin{aligned} &\|S\| \left\{ \sqrt{2\left(\frac{1}{m_v^2} + \frac{1}{m_0^2}\right)\left\{k_e^2 + c_e^2\right\}} + \frac{k_v}{m_v} \right\} < k'' \\ &0 < \alpha < 1 \end{aligned} \tag{38}$$

A significant problem that sometimes occurs in SMC systems is chattering due to a discontinuous switching input [36], [44]. To prevent chattering, the signum function $sgn(\sigma)$ is smoothed by an approximation using the hyperbolic tangent [45]–[48]. Consequently, (39) shows the control input used in the simulations and experiments. Here, δ is a small positive parameter for smoothing.

$$\begin{aligned} u &= u_l + u_{nl} \\ &= -(SB_{v2})^{-1} SA_{vn} x_{va} \\ &\quad - k''\,(SB_{v2})^{-1}\,|\sigma|^{\alpha}\,\|x_{va}\|\, Tanh\left(\frac{\sigma}{\delta}\right) \end{aligned} \tag{39}$$

Fig. 4 shows the block diagram of the proposed control scheme.

For the numerical calculations in the controller design, this study employs Control System Toolbox and Robust Control Toolbox of MATLAB. Table 2 shows the parameters for designing the sliding surface and control input. Specifically, they were determined by actually conducting simulations and experiments and confirming the results demonstrated later. Some trial-and-error adjustments were also necessary. These parameters are used in both the simulations and experiments below.

IV. SIMULATION STUDY

A. CONFIGURATION OF THE SIMULATION

A simulation study was conducted to verify the vibration suppression performance and robustness to the actuator's parameter uncertainty of the proposed method. From our previous study [35] applying H_∞ control to compensate for the

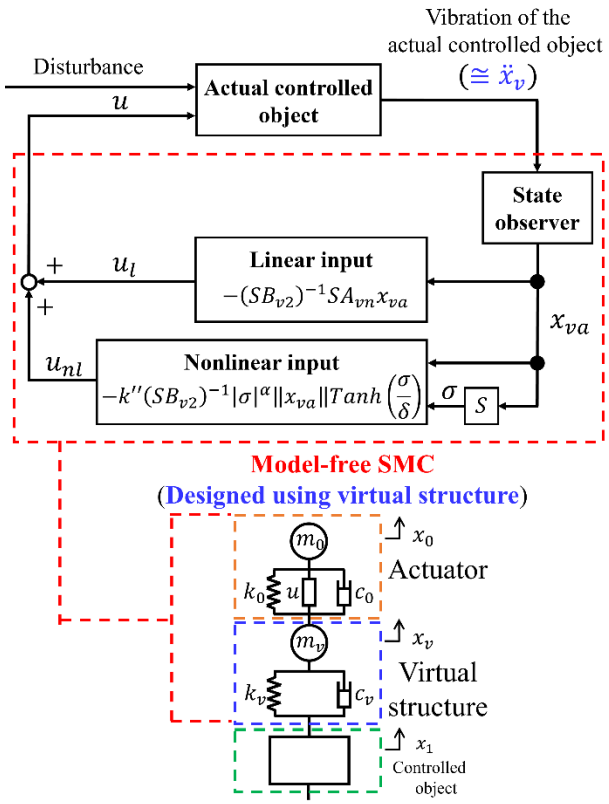

FIGURE 4. The block diagram of the proposed control scheme.

TABLE 2. Parameters used for designing the sliding mode controller.

Properties	Value
W	$diag\{10^{-20} \quad 10^{-20} \quad 10^{-20} \quad 10^{-30}\}$
k''	1.0×10^{1}
δ	5.0×10^{-5}
α	1.2×10^{-2}

actuator uncertainty, the following problem has been already revealed. Hence, one of the goals of this paper is to solve the following problem.

- Depending on the amount of the actuator uncertainty, the H_∞ controller becomes too conservative, resulting in insufficient damping performances.

The principal purpose of the simulation studies is to confirm that the application of SMC can solve the above problem compared to our previous paper employing H_∞ control. That is, the simulation study was conducted to demonstrate that the proposed model-free SMC improves the damping performance and robustness with respect to the actuator uncertainty, compared to a conservative H_∞ controller. Especially, the actuator uncertainty satisfies the matching condition in the model-free SMC designed based on the virtual structure. It means that we can utilize the specific advantage of SMC which cannot be obtained by a H_∞ controller in contrast. Fig. 5 shows the controlled object as a 2DOF system, which is a time-varying system where both masses m_1 and m_2

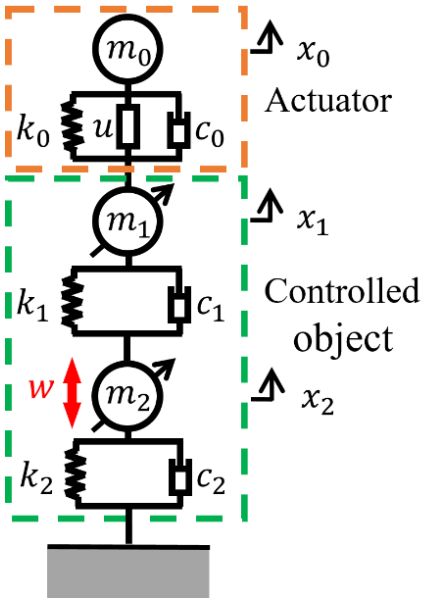

FIGURE 5. Simulation setup.

TABLE 3. Parameters for the 2DOF time-varying controlled object.

Properties	Value	Unit
m_1, m_2	3.6 ± 0.72 (time-varying)	kg
k_1, k_2	1.0×10^{6}	N/m
c_1, c_2	1.9×10^{1}	Ns/m

fluctuate sinusoidally in the range of $\pm 20\%$. Table 3 shows the model parameters. The goal of the simulation was to suppress the vibration of point mass m_1 when point mass m_2 was excited by a white noise disturbance. Upon changing the actuator's stiffness and damping, the vibration suppression performance and robustness to the actuator's parameter uncertainty were evaluated by the vibration control simulation using the sliding mode controller designed by the proposed method (SM Controller). The proposed method was compared with the H_∞ controller designed for the system (6)–(8) considering the actuator's uncertainty (Hinf Controller), which is proposed in the previous study [35]. In this study, the actuator's parameter uncertainty range to be considered was $\pm 50\%$.

In this simulation study, the vibration suppression performance was evaluated by the performance index L shown in (40) [11], [12], [14].

$$L_i = \frac{1}{f_s} \sum_{k=(i-1)n+1}^{in} (y[k])^2 \quad i = 1, 2, \cdots \tag{40}$$

Here, L_i indicates the performance index in the i-th evaluation interval. $y[k]$ represents the observed output at the k-th sampling point from the start of the simulation and is the acceleration of the point mass m_1. n represents the number of evaluation points in each evaluation interval. f_s is the sampling frequency. Consequently, performance index L represents the mean-square value in each evaluation interval. In this study, n and f_s were set as 1000 points and 20 kHz,

respectively. All simulations used the same mean and variance values for the white noise disturbance.

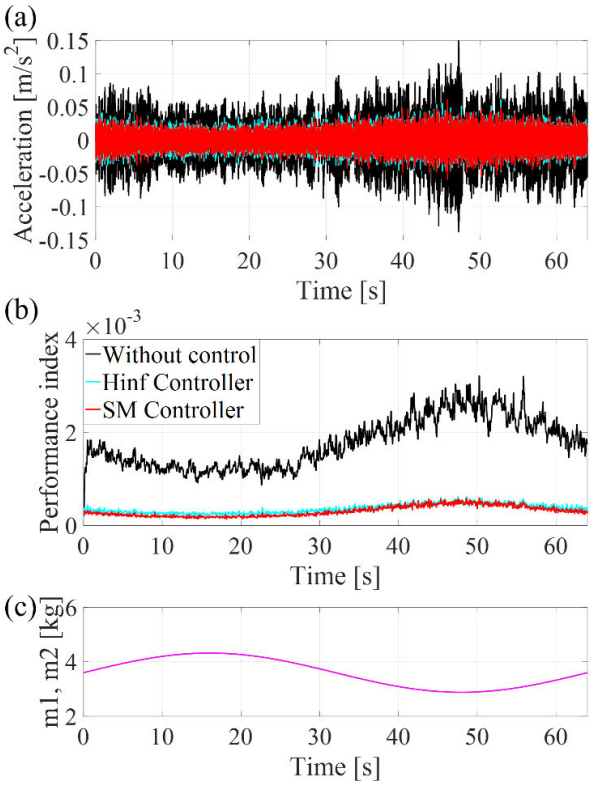

FIGURE 6. Simulation results (*ErK* : 0% *ErC* : 0%): (a) Acceleration; (b) Performance index; (c) Mass variations of m_1 and m_2.

B. VIBRATION CONTROL SIMULATION RESULTS AND DISCUSSION

Figs. 6 and 7 show the results for an average of 50 simulations. The black, blue, and red lines depict the time history response without control, the result from the Hinf controller, and the result from the SM controller, respectively. The symbols *ErK* and *ErC* indicate that the actual values during the simulation have errors of *ErK* [%] and *ErC* [%], respectively, for normal actuator stiffness and damping shown in Table 1. Figs 6(c) and 7(c) show the time histories of the variations of the masses m_1 and m_2.

Both the Hinf controller and SM controller provided sufficient vibration performance because the actuator did not have errors (Fig. 6). However, the SM controller realized a sufficient damping performance, whereas that for the Hinf controller significantly deteriorated around 30 s even though neither controller was destabilized (Fig. 7). This difference was attributed to the matching uncertainty (uncertainty of the actuator), which is unique to the sliding mode controller designed in Chapter 3. Consequently, the proposed method achieved a performance superior to previous studies using H_∞ control theory [35] in terms of robustness to the actuator's parameter uncertainty. In addition, the simulations demonstrated the applicability of the proposed method to time-varying systems.

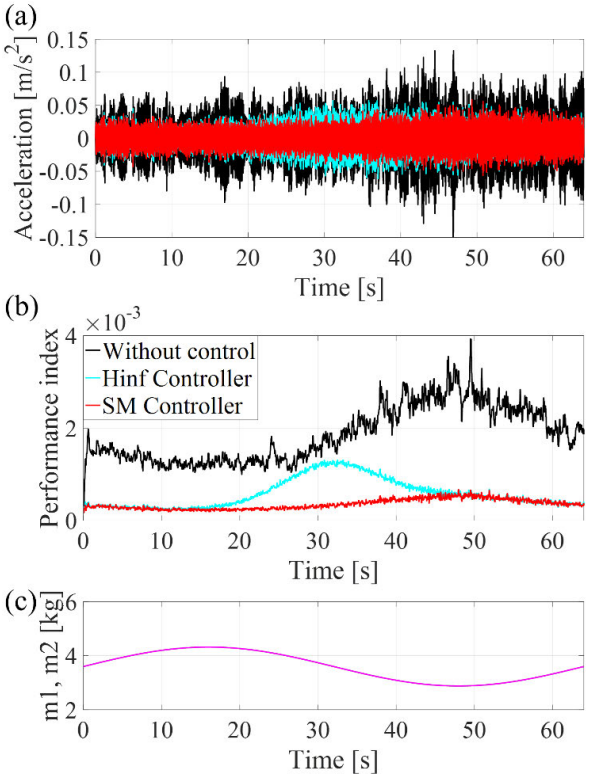

FIGURE 7. Simulation results (*ErK* : 50% *ErC* : −50%): (a) Acceleration; (b) Performance index; (c) Mass variations of m_1 and m_2.

V. EXPERIMENTAL VERIFICATIONS

A. CONFIGURATION OF THE EXPERIMENTAL SYSTEM

The vibration control experiment was conducted for demonstrating the applicability of the proposed method to actual mechanical systems. Fig. 8 shows the experimental system. Figs. 8(a) and (b) show the controlled objects employed in the experimental verifications. (a) is a both ends supported plate, and (b) is a cantilever plate. The controlled object in Fig. 8(a) (hereafter named as "Controlled object 1") was composed of aluminum with a size of 548 × 100 × 10 mm. The controlled object in Fig. 8(b) (hereafter named as "Controlled object 2") was with a size of 190 × 248 × 10 mm and made of the same material as Controlled object 1. A load cell was mounted at position A to measure the disturbance force applied by the shaker. The control input was applied by the actuator mounted at position B. The observed output was measured by an accelerometer attached to C on the back side of the plate at the same location as the actuator. Figs. 8(c) and 8(d) show a closed-loop system and the actual experimental system, respectively. The observed output was acquired by the accelerometer and inputted to the digital signal processor (DSP). The control input command value calculated by the DSP passed through an analog low-pass filter (Order: 4, Type: Butterworth) to prevent spillover, and then was amplified by the current amplifier to drive the actuator. As a disturbance, a 1–1000 Hz linear sweep sinusoidal signal was delivered from the signal generator. The spectrum analyzer calculated

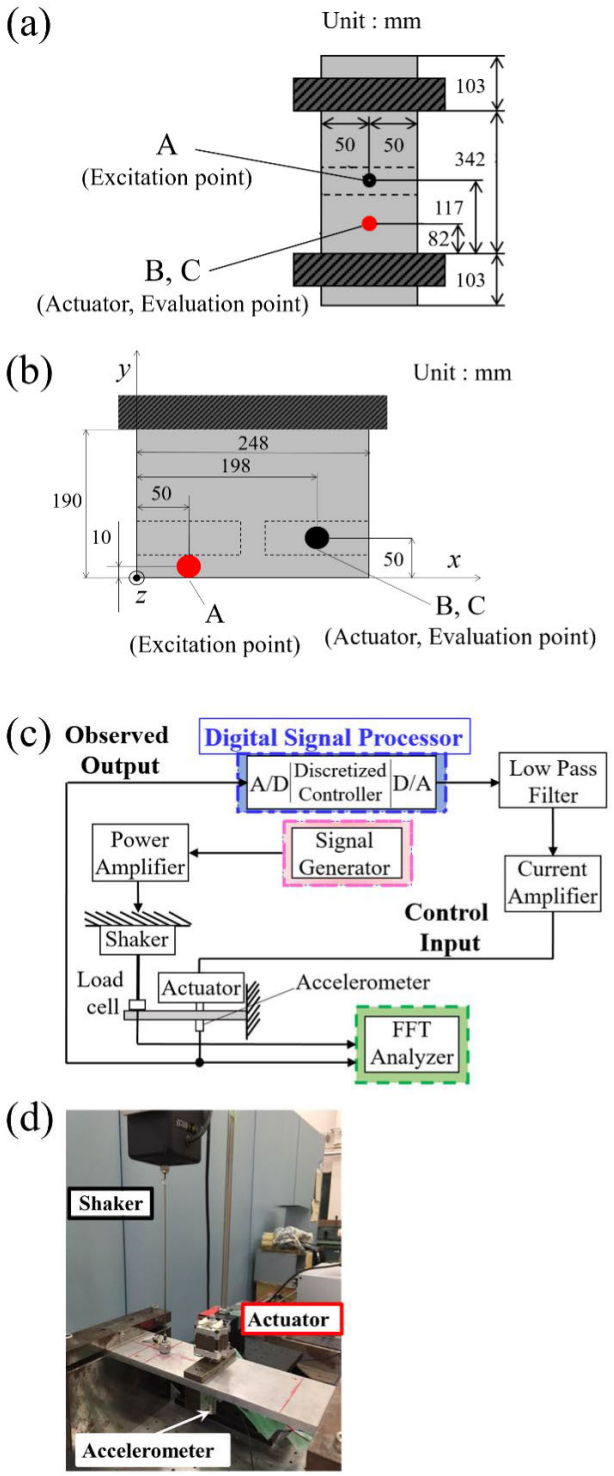

FIGURE 8. Experimental system: (a) Overview of the controlled object (Controlled object 1); (b) Overview of the controlled object (Controlled object 2); (c) System diagram; (d) Experimental setup.

the frequency response from the disturbance (load cell) to the observed output (acceleration obtained from the sensor). That is, the vibration suppression performance was evaluated based on the acceleration of the controlled object. The control bandwidth in this study was set between 50 and 1000 Hz.

In design of the model-free SMC, the same values of the parameters as those in Table 2 were consistently used in all of the experimental verifications demonstrated later. The error range of the actuator's parameters to be compensated was set as $\pm 50\%$.

B. VIBRATION CONTROL EXPERIMENT TO CONFIRM THE ROBUSTNESS TO THE ACTUATOR'S UNCERTAINTY

The purpose of the experiments in this section is to verify that the proposed model-free SMC can achieve sufficient damping performances even though the actuator's parameters uncertainties are induced. The controlled objects are shown in Fig. 8(a) and (b).

It was difficult to prepare multiple actuators with varying parameters for experiments. Therefore, in this study, the parameters of the actuator model shown in Table 1, which are defined as nominal in the controller design stage, are varied. By designing a controller with this actuator model, situations where parameter errors occur for the unique actuator used in the experiment can be created equivalently. The error range of the actuator's parameters to be compensated was $\pm 50\%$. Based on the method presented in Chapter 3, sliding mode controllers were designed using various parameters of the actuator, and vibration control experiments are conducted on Controlled objects 1 and 2. Table 2 shows the tuning parameters used to design the sliding mode controller.

Figs. 9–12 show the representative results of the vibration control experiments, which are the frequency responses of the acceleration from the disturbance to the observed output. The black and red lines indicate the frequency response without control and the closed-loop frequency response with control, respectively. ErK and ErC represent that the stiffness and damping of the actuator parameters employed in the experiment had errors of ErK [%] and ErC [%], respectively, with respect to the stiffness and damping of the actuator used for controller design. Tables 4 and 5 shows the main damping results for various errors of the actuator parameters.

TABLE 4. Results of the vibration control experiments with Controlled object 1.

Parameters of Actuator Value		Reduction amount[dB]
ErK[%]	ErC[%]	226Hz peak
0	0	−15.1
50	50	−15.0
−50	50	−14.6
50	−50	−14.9
−50	−50	−14.7

C. MODEL-FREE SMC VS. MODEL-BASED SMC

SMC proposed in this study becomes a model-free controller which is designed based on the idea of virtual structure. Because this design method does not depend on the specific models of actual controlled object, the controller has robustness against a complete change of a controlled object.

TABLE 5. Results of the vibration control experiments with Controlled object 2.

Parameters of Actuator Value		Reduction amount[dB]	
ErK[%]	ErC[%]	117Hz peak	273Hz peak
0	0	−9.5	−9.4
50	50	−10.0	−6.7
−50	50	−8.3	−7.3
50	−50	−9.8	−6.6
−50	−50	−9.7	−6.5

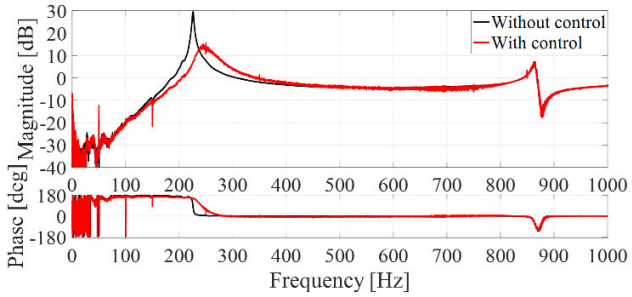

FIGURE 9. Frequency response obtained in the experiments with Controlled object 1 (*ErK* : 0% *ErC* : 0%).

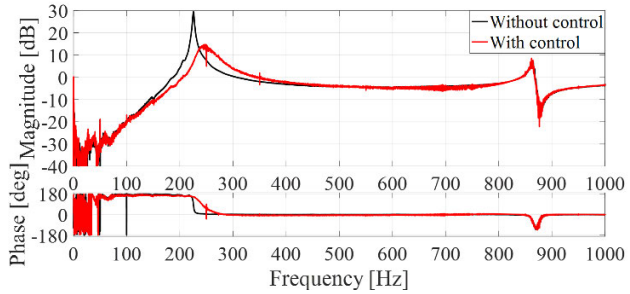

FIGURE 10. Frequency response obtained in the experiments with Controlled object 1 (*ErK* : 50% *ErC* : −50%).

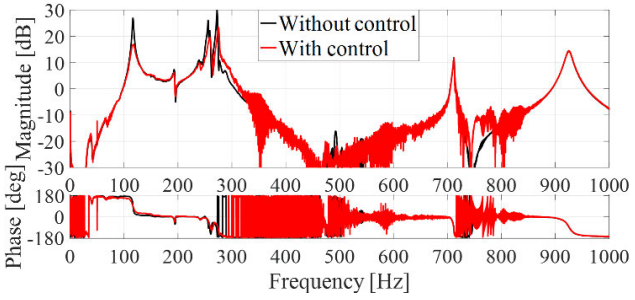

FIGURE 11. Frequency response obtained in the experiments with Controlled object 2 (*ErK* : 50% *ErC* : 50%).

To verify this advantage, comparative experiments were performed. From the purpose of the experiments, a conventional SMC [36], which is designed using a model of a controlled object, was chosen to compare. The controlled object model shown in Fig. 13 was used to design the conventional SMC.

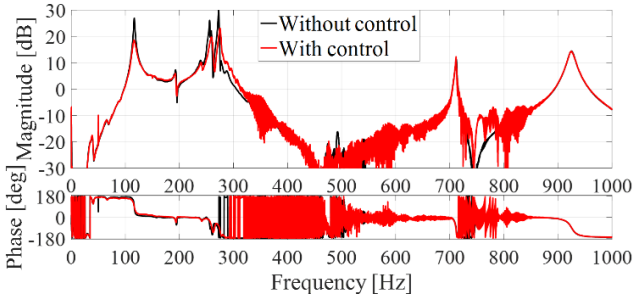

FIGURE 12. Frequency response obtained in the experiments with Controlled object 2 (*ErK* : −50% *ErC* : 50%).

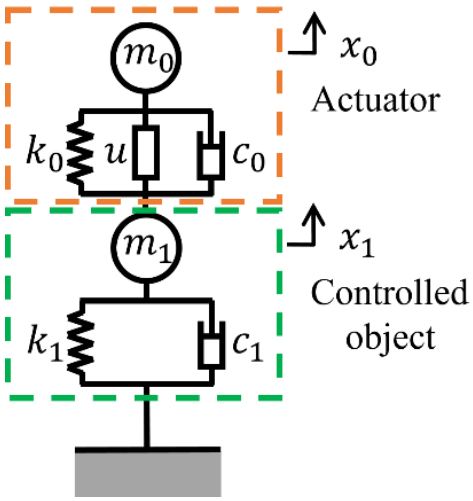

FIGURE 13. Model used for the MBSMC design and the vibration control simulations for MBSMC and MFSMC.

Fig. 13 describes the vibration system composed of the actuator and the SDOF controlled object. As model parameters, m_1[kg], k_1[N/m], and c_1[Ns/m] were set as 1.2, 1.0×10^6, and 10.95, respectively [35].

Consequently, vibration control experiments were conducted for both the model-free SMC (“MFSMC”) designed via the proposed approach without using any models of controlled objects and the model-based SMC (“MBSMC”) designed using the controlled object model shown in Fig. 13. The concrete procedures of the comparative experiments are indicated as follows.

1. MBSMC, which should be compared with the proposed MFSMC, is designed using the model of SDOF controlled object shown in Fig. 13 [36]. On the other hand, MFSMC can be obtained from the proposed model-free design described in Chapters 2 and 3.
2. For the controlled object model shown in Fig. 13, which was used to design MBSMC, vibration control simulation is performed. In this simulation, MBSMC is tuned so that the performance of MBSMC becomes the same as that of MFSMC. For proper comparison in steps 3 and 4 later, the initial performances of MBSMC and MFSMC should be equal.

3. Next, the comparative experiments are conducted. For both MFSMC and MBSMC, the controllers, which are exactly same, including the values of the tuning parameters, as those used for the simulations in step 2, are applied to the controlled object shown in Fig. 8(b), respectively. In other words, for each of MFSMC and MBSMC, the control experiment is performed for "Controlled object 2" (cantilever plate) using exactly the same controller as one applied to SDOF controlled object shown in Fig. 13 in step 2.
4. Then, the damping performance of MFSMC is compared with that of MBSMC.

The reason why MBSMC was designed for the SDOF controlled object shown Fig. 13 is because making the performance of MBSMC the same as MFSMC in step 2 is easy.

Note that all of the experiments in Section 5.C. used the same model-free sliding mode controller, which was obtained using the parameters presented in Table 2. This verification methodology is aimed at confirming that the model-free controller, which does not depend on models of controlled objects, has robustness against various different structures. Consequently, for the controller via the proposed design method and the controller via the conventional model-based sliding mode control theory [36], their damping performances are experimentally compared when a controlled object completely changes.

Figs. 14 and 15 show the comparative verification results. Fig. 14 is the result where the vibration control simulation was performed for both MFSMC and MBSMC in step 2 and their damping performances are almost equal. Fig. 15 demonstrates the experimental results for Controlled object 2 (i.e. cantilever plate) in step 3. In Figs. 14 and 15, the blue and red lines indicate the control results by MBSMC and MFSMC, respectively. The black line represents the open-loop responses without control.

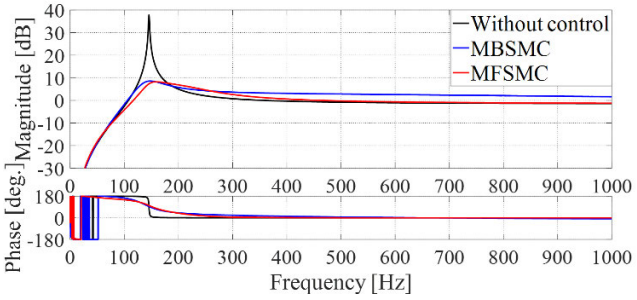

FIGURE 14. Frequency response obtained in the simulations for MBSMC and MFSMC. MBSMC achieved almost the same performance as that of MFSMC.

D. DISCUSSION

In Section 5.B., despite the uncertainty in the actuator's parameters, a sufficient damping effect was achieved for the major vibration modes in the control frequency band (Figs. 9–12, Tables 4 and 5). Hence, the controller achieved

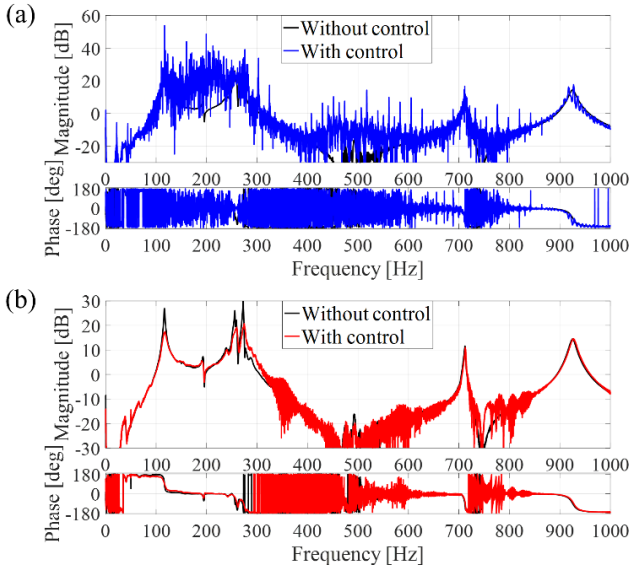

FIGURE 15. Frequency response obtained in the experiments with Controlled object 2 (cantilever plate): (a) result by MBSMC; (b) result by MFSMC.

a damping effect without instability despite errors of ±50% in the stiffness and damping of the actuator because the parameter error of the actuator satisfied the matching condition described in Section 3.C. This is one of the advantages obtained by the application of SMC to the model-free design based on virtual structure. That is, it is noteworthy contribution that the robustness to the actuator uncertainty can be ensured with the model-free controller design simultaneously. Consequently, the model-free sliding mode controller designed using the proposed method has a high damping effect on actual mechanical structures.

Below, we discuss the comparative verification results in Section 5.C.

As demonstrated in Fig. 14, the damping performance of MBSMC becomes the same as that of MFSMC. That is, in the control simulations for the controlled object shown in Fig. 13, the performances of MBSMC and MFSMC are almost equal. Consequently, Fig. 14 confirmed that both MFSMC and MBSMC achieved the proper vibration suppression for the structure shown in Fig. 13.

On the other hand, in the vibration control experiments for the Controlled object 2 (i.e. cantilever plate), which is completely different from the model used to design MBSMC, MFSMC achieves the sufficient damping effects as shown in Fig. 15(b) even though the closed-loop system with MBSMC is destabilized as shown in Fig. 15(a). In Fig. 15(b), MFSMC provides the high damping effects for the major peaks in 1–400 Hz.

This is because the proposed controller (MFSMC) is designed without detailed mathematical models of the actual structures and is less susceptible to structure changes. In other words, the proposed design approach using virtual structure has an advantage that it does not depend on the specific

structures of controlled objects. On the other hand, as shown in Fig. 15(a), since MBSMC is a model-based controller, it is difficult to control a controlled object that is completely different from the model used to design the controller. Consequently, the comparative experimental results demonstrated that the model-free SMC designed using the proposed method can realize high vibration suppression performance even when the controlled object is changed while SMC designed with the conventional model-based control approach cannot deal with it.

Throughout this study, structures with significantly different characteristics were controlled in both the vibration control simulations and experiments, demonstrating effective vibration suppression for all structures. The model-free controller used in all of the simulations and experiments has the same design parameters listed in Table 2. This fact confirmed that it possessed a high damping effect on structures with various characteristics.

VI. CONCLUSION

The purpose of this study was to construct a model-free active vibration control technique considering actuator's parameter uncertainty using an actuator model including a virtual structure and sliding mode control theory. The proposed method indirectly suppresses vibration without a model of the actual controlled object by inserting a virtual structure defined as a SDOF system between the actuator model and the controlled object. The actuator's parameter uncertainty was modelled quantitatively so as to achieve the robustness to the actuator's uncertainty. It was proved that the actuator's parameter uncertainty in the model-free vibration control system using the virtual structure satisfies the matching condition of sliding mode control theory. A sliding surface which minimizes the fluctuations of the state on the sliding surface was designed for the system composed of the actuator and virtual structure. Using the Lyapunov function for the dynamics of the switching function, the control input and the condition for the existence of the sliding mode are derived. The effectiveness of the proposed technique was confirmed by both simulations to the time-varying system and experiments to the both ends supported plate and the cantilever plate. As a result, high robustness with the actuator's parameter uncertainty, which satisfies the matching condition, which originates from the nature of sliding mode control, was confirmed. In addition, the applicability to time-varying systems and sufficient damping effect to the actual mechanical system of the proposed method were revealed. In addition, the conventional model-based SMC and the model-free SMC designed using the proposed method were compared in the vibration control experiment. The results confirmed the advantage (i.e. the robustness against the changing of the controlled object) of the model-free controller proposed in this study.

In the future, vibration control experiments to time-varying systems will be conducted and its applicability will be verified. Moreover, the proposed vibration control scheme will be improved so that the bound information of the uncertainties is not needed. This issue may be solved by introducing an adaptive scheme.

REFERENCES

[1] A. Parameswaran, A. Pai, P. Tripathi, and K. Gangadharan, "Active vibration control of a smart cantilever beam on general purpose operating system," *Defence Sci. J.*, vol. 63, no. 4, pp. 413–417, Jul. 2013.
[2] M. Kant and A. P. Parameswaran, "Modeling of low frequency dynamics of a smart system and its state feedback based active control," *Mech. Syst. Signal Process.*, vol. 99, pp. 774–789, Jan. 2018.
[3] W. Wang, Y. Li, J. Shi, and C. Lin, "Vibration control method for an electric city bus driven by a dual motor coaxial series drive system based on model predictive control," *IEEE Access*, vol. 6, pp. 41188–41200, 2018.
[4] Z. Lin, S. Lin, S. Wu, G. Ma, and Z. Liang, "Vibration control of a flexible spacecraft system with input backlash," *IEEE Access*, vol. 7, pp. 87017–87026, 2019.
[5] T. Meurers, S. M. Veres, and A. C. H. Tan, "Model-free frequency domain iterative active sound and vibration control," *Control Eng. Pract.*, vol. 11, no. 9, pp. 1049–1059, Sep. 2003.
[6] G. G. Rigatos, "Model-based and model-free control of flexible-link robots: A comparison between representative methods," *Appl. Math. Model.*, vol. 33, no. 10, pp. 3906–3925, Oct. 2009.
[7] C. Wei, J. Luo, H. Dai, and J. Yuan, "Adaptive model-free constrained control of postcapture flexible spacecraft: A Euler–Lagrange approach," *J. Vib. Control*, vol. 24, no. 20, pp. 4885–4903, Oct. 2018.
[8] S. Ahmed, H. Wang, and Y. Tian, "Model-free control using time delay estimation and fractional-order nonsingular fast terminal sliding mode for uncertain lower-limb exoskeleton," *J. Vib. Control*, vol. 24, no. 22, pp. 5273–5290, Nov. 2018.
[9] J. Swevers, C. Lauwerys, B. Vandersmissen, M. Maes, K. Reybrouck, and P. Sas, "A model-free control structure for the on-line tuning of the semi-active suspension of a passenger car," *Mech. Syst. Signal Process.*, vol. 21, no. 3, pp. 1422–1436, Apr. 2007.
[10] A. Boubakir, S. Labiod, and F. Boudjema, "A stable self-tuning proportional-integral-derivative controller for a class of multi-input multi-output nonlinear systems," *J. Vib. Control*, vol. 18, no. 2, pp. 228–239, Feb. 2012.
[11] K. Furuya, S. Ishizuka, and I. Kajiwara, "Online tuning of a model-based controller by perturbation of its poles," *J. Adv. Mech. Des. Syst. Manuf.*, vol. 9, no. 2, pp. 1–12, 2015.
[12] S. Ishizuka and I. Kajiwara, "Online adaptive PID control for MIMO systems using simultaneous perturbation stochastic approximation," *J. Adv. Mech. Des. Syst. Manuf.*, vol. 9, no. 2, pp. 1–16, 2015.
[13] K. Butt and N. Sepehri, "Model-free online tuning of controller parameters using a globalized local search algorithm," *Optim. Control Appl. Methods*, vol. 39, no. 5, pp. 1750–1765, Sep. 2018.
[14] I. Kajiwara, K. Furuya, and S. Ishizuka, "Experimental verification of a real-time tuning method of a model-based controller by perturbations to its poles," *Mech. Syst. Signal Process.*, vol. 107, pp. 396–408, Jul. 2018.
[15] A. Safaei and M. N. Mahyuddin, "Adaptive model-free control based on an ultra-local model with model-free parameter estimations for a generic SISO system," *IEEE Access*, vol. 6, pp. 4266–4275, 2018.
[16] Y.-L. Zhou, Q.-Z. Zhang, X.-D. Li, and W.-S. Gan, "On the use of an SPSA-based model-free feedback controller in active noise control for periodic disturbances in a duct," *J. Sound Vib.*, vol. 317, nos. 3–5, pp. 456–472, Nov. 2008.
[17] Y. Zheng, N. Mo, Y. Zhou, and Z. Shi, "A model-free control method for synchronous vibration of active magnetic bearing rotor system," *IEEE Access*, vol. 7, pp. 79254–79267, 2019.
[18] S. Yahagi, I. Kajiwara, and T. Shimozawa, "Slip control during inertia phase of clutch-to-clutch shift using model-free self-tuning proportional-integral-derivative control," *Proc. Inst. Mech. Eng., D, J. Automobile Eng.*, vol. 234, no. 9, pp. 2279–2290, Aug. 2020.
[19] K. Deng, F. Li, and C. Yang, "A new data-driven model-free adaptive control for discrete-time nonlinear systems," *IEEE Access*, vol. 7, pp. 126224–126233, 2019.
[20] S. D. Snyder and N. Tanaka, "Active control of vibration using a neural network," *IEEE Trans. Neural Netw.*, vol. 6, no. 4, pp. 819–828, Jul. 1995.
[21] Ş. Yildirim, "Vibration control of suspension systems using a proposed neural network," *J. Sound Vib.*, vol. 277, nos. 4–5, pp. 1059–1069, Nov. 2004.
[22] Q.-Z. Zhang and W.-S. Gan, "Active noise control using a simplified fuzzy neural network," *J. Sound Vib.*, vol. 272, nos. 1–2, pp. 437–449, Apr. 2004.

[23] A. Madan, "Vibration control of building structures using self-organizing and self-learning neural networks," *J. Sound Vib.*, vol. 287, nos. 4–5, pp. 759–784, Nov. 2005.
[24] S. M. Yang, C. J. Chen, and W. L. Huang, "Structural vibration suppression by a neural-network controller with a mass-damper actuator," *J. Vib. Control*, vol. 12, no. 5, pp. 495–508, May 2006.
[25] H. Yousefi, M. Hirvonen, H. Handroos, and A. Soleymani, "Application of neural network in suppressing mechanical vibration of a permanent magnet linear motor," *Control Eng. Pract.*, vol. 16, no. 7, pp. 787–797, Jul. 2008.
[26] Q. Zhang, S. Wang, A. Zhang, J. Zhou, and Q. Liu, "Improved PI neural network-based tension control for stranded wire helical springs manufacturing," *Control Eng. Pract.*, vol. 67, pp. 31–42, Oct. 2017.
[27] O. Abdeljaber, O. Avci, and D. J. Inman, "Active vibration control of flexible cantilever plates using piezoelectric materials and artificial neural networks," *J. Sound Vib.*, vol. 363, pp. 33–53, Feb. 2016.
[28] V. G. Moudgal, W. A. Kwong, K. M. Passino, and S. Yurkovich, "Fuzzy learning control for a flexible-link robot," *IEEE Trans. Fuzzy Syst.*, vol. 3, no. 2, pp. 199–210, May 1995.
[29] M. Malhis, L. Gaudiller, and J. Der Hagopian, "Fuzzy modal active control of flexible structures," *J. Vib. Control*, vol. 11, no. 1, pp. 67–88, Jan. 2005.
[30] S. Edalath, A. R. Kukreti, and K. Cohen, "Enhancement of a tuned mass damper for building structures using fuzzy logic," *J. Vib. Control*, vol. 19, no. 12, pp. 1763–1772, Sep. 2013.
[31] C. Song, Z. Zhou, S. Xie, Y. Hu, J. Zhang, and H. Wu, "Fuzzy control of a semi-active multiple degree-of-freedom vibration isolation system," *J. Vib. Control*, vol. 21, no. 8, pp. 1608–1621, Jun. 2015.
[32] S. Thenozhi and W. Yu, "Active vibration control of building structures using fuzzy proportional-derivative/proportional-integral-derivative control," *J. Vib. Control*, vol. 21, no. 12, pp. 2340–2359, Sep. 2015.
[33] H. Yonezawa, I. Kajiwara, and A. Yonezawa, "Model-free vibration control to enable vibration suppression of arbitrary structures," in *Proc. 12th Asian Control Conf.*, Jun. 2019, pp. 289–294.
[34] H. Yonezawa, I. Kajiwara, and A. Yonezawa, "Experimental verification of model-free active vibration control approach using virtually controlled object," *J. Vib. Control*, vol. 26, nos. 19–20, pp. 1656–1668, 2020.
[35] A. Yonezawa, I. Kajiwara, and H. Yonezawa, "Model-free vibration control based on a virtual controlled object considering actuator uncertainty," *J. Vib. Control*, Jul. 2020, Art. no. 107754632094092, doi: 10.1177/1077546320940922.
[36] Y. Shtessel, C. Edwards, L. Fridman, and A. Levant, *Sliding Mode Control and Observation*. Basel, Switzerland: Birkhäuser, 2014.
[37] X. Yu and O. Kaynak, "Sliding-mode control with soft computing: A survey," *IEEE Trans. Ind. Electron.*, vol. 56, no. 9, pp. 3275–3285, Jul. 2009.
[38] J. Yang, S. Li, and X. Yu, "Sliding-mode control for systems with mismatched uncertainties via a disturbance observer," *IEEE Trans. Ind. Electron.*, vol. 60, no. 1, pp. 160–169, Jan. 2013.
[39] W. Deng and J. Yao, "Asymptotic tracking control of mechanical servosystems with mismatched uncertainties," *IEEE/ASME Trans. Mechatronics*, early access, Oct. 30, 2020, doi: 10.1109/TMECH.2020.3034923.
[40] W. Deng and J. Yao, "Extended-state-observer-based adaptive control of electrohydraulic servomechanisms without velocity measurement," *IEEE/ASME Trans. Mechatronics*, vol. 25, no. 3, pp. 1151–1161, Jun. 2020.
[41] B. Lu, Y. Fang, and N. Sun, "Continuous sliding mode control strategy for a class of nonlinear underactuated systems," *IEEE Trans. Autom. Control*, vol. 63, no. 10, pp. 3471–3478, Oct. 2018.
[42] A. H. Khan and S. Li, "Sliding mode control with PID sliding surface for active vibration damping of pneumatically actuated soft robots," *IEEE Access*, vol. 8, pp. 88793–88800, 2020.
[43] M. A. Eshag, L. Ma, Y. Sun, and K. Zhang, "Robust global boundary vibration control of uncertain timoshenko beam with exogenous disturbances," *IEEE Access*, vol. 8, pp. 72047–72058, 2020.
[44] K. D. Young, V. I. Utkin, and U. Ozguner, "A control engineer's guide to sliding mode control," *IEEE Trans. Control Syst. Technol.*, vol. 7, no. 3, pp. 328–342, May 1999.
[45] G. Song and H. Gu, "Active vibration suppression of a smart flexible beam using a sliding mode based controller," *J. Vib. Control*, vol. 13, no. 8, pp. 1095–1107, Aug. 2007.
[46] A. P. Parameswaran, B. Ananthakrishnan, and K. V. Gangadharan, "Modeling and design of field programmable gate array based real time robust controller for active control of vibrating smart system," *J. Sound Vib.*, vol. 345, pp. 18–33, Jun. 2015.
[47] A. P. Parameswaran, B. Ananthakrishnan, and K. V. Gangadharan, "Design and development of a model free robust controller for active control of dominant flexural modes of vibrations in a smart system," *J. Sound Vib.*, vol. 355, pp. 1–18, Oct. 2015.
[48] I. Yiğit, "Model free sliding mode stabilizing control of a real rotary inverted pendulum," *J. Vib. Control*, vol. 23, no. 10, pp. 1645–1662, 2017.

ANSEI YONEZAWA received the B.S. degree in mechanical engineering from Hokkaido University, in 2019, where he is currently pursuing the M.S. degree with the Graduate School of Engineering. He received the Hatakeyama Prize given for best students in the field of mechanical engineering from the Japan Society of Mechanical Engineers in 2019. His research interests include active vibration control, robust control, and stochastic optimization.

ITSURO KAJIWARA received the B.S. degree in engineering from Tokyo Metropolitan University, in 1986, and the M.S. and Ph.D. degrees in engineering from the Tokyo Institute of Technology, in 1988 and 1993, respectively. From 1990 to 2000, he was an Assistant Professor with the School of Engineering, Tokyo Institute of Technology, where he was an Associate Professor with the Graduate School of Engineering, from 2000 to 2008. Since 2009, he has been a Professor with the Graduate School of Engineering, Hokkaido University. His research interests include vibration, control, structural health monitoring, and laser application.

HEISEI YONEZAWA received the B.S. and M.S. degrees in mechanical engineering from Hokkaido University, in 2017 and 2019, respectively, where he is currently pursuing the Ph.D. degree with the Graduate School of Engineering. He received the Miura Prize given for best students in the field of mechanical engineering from the Japan Society of Mechanical Engineers in 2019. His research interests include powertrain control, vibration control, and sampled-data control.